

UCLA

UCLA Previously Published Works

Title

Hybrid hydrogels containing vertically aligned carbon nanotubes with anisotropic electrical conductivity for muscle myofiber fabrication.

Permalink

<https://escholarship.org/uc/item/4tt0404j>

Journal

Scientific reports, 4(1)

ISSN

2045-2322

Authors

Ahadian, Samad
Ramón-Azcón, Javier
Estili, Mehdi
[et al.](#)

Publication Date

2014-03-01

DOI

10.1038/srep04271

Peer reviewed



OPEN

SUBJECT AREAS:

BIOMEDICAL
ENGINEERING

TISSUE ENGINEERING

Hybrid hydrogels containing vertically aligned carbon nanotubes with anisotropic electrical conductivity for muscle myofiber fabrication

Received
9 September 2013Accepted
13 February 2014Published
19 March 2014

Correspondence and requests for materials should be addressed to T.M. (matsue@bioinfo.che.tohoku.ac.jp) or A.K. (alik@rics.bwh.harvard.edu)

* These authors contributed equally to this work.

Samad Ahadian^{1*}, Javier Ramón-Azcón^{1*}, Mehdi Estili², Xiaobin Liang¹, Serge Ostrovidov¹, Hitoshi Shiku³, Murugan Ramalingam^{1,4,5}, Ken Nakajima¹, Yoshio Sakka⁶, Hojae Bae⁷, Tomokazu Matsue^{1,3} & Ali Khademhosseini^{1,8,9,10,11}

¹WPI-Advanced Institute for Materials Research, Tohoku University, Sendai 980-8577, Japan, ²International Center for Young Scientists (ICYS), National Institute for Materials Science (NIMS), Tsukuba 305-0047, Japan, ³Graduate School of Environmental Studies, Tohoku University, Sendai 980-8579, Japan, ⁴Centre for Stem Cell Research, A unit of the Institute for Stem Cell Biology and Regenerative Medicine, Christian Medical College Campus, Vellore 632002, India, ⁵Institut National de la Santé Et de la Recherche Médicale U977, Faculté de Chirurgie Dentaire, Université de Strasbourg, Strasbourg 67085, France, ⁶Materials Processing Unit, National Institute for Materials Science (NIMS), Tsukuba 305-0047, Japan, ⁷College of Animal Bioscience and Technology, Department of Bioindustrial Technologies, Konkuk University, Hwayang-dong, Kwangjin-gu, Seoul 143-701, Republic of Korea, ⁸Department of Medicine, Center for Biomedical Engineering, Brigham and Women's Hospital, Harvard Medical School, Cambridge, Massachusetts 02139, USA, ⁹Harvard-MIT Division of Health Sciences and Technology, Massachusetts Institute of Technology, Cambridge, Massachusetts 02139, USA, ¹⁰Wyss Institute for Biologically Inspired Engineering, Harvard University, Boston, Massachusetts 02115, USA, ¹¹Department of Maxillofacial Biomedical Engineering and Institute of Oral Biology, School of Dentistry, Kyung Hee University, Seoul 130-701, Republic of Korea.

Biological scaffolds with tunable electrical and mechanical properties are of great interest in many different fields, such as regenerative medicine, biorobotics, and biosensing. In this study, dielectrophoresis (DEP) was used to vertically align carbon nanotubes (CNTs) within methacrylated gelatin (GelMA) hydrogels in a robust, simple, and rapid manner. GelMA-aligned CNT hydrogels showed anisotropic electrical conductivity and superior mechanical properties compared with pristine GelMA hydrogels and GelMA hydrogels containing randomly distributed CNTs. Skeletal muscle cells grown on vertically aligned CNTs in GelMA hydrogels yielded a higher number of functional myofibers than cells that were cultured on hydrogels with randomly distributed CNTs and horizontally aligned CNTs, as confirmed by the expression of myogenic genes and proteins. In addition, the myogenic gene and protein expression increased more profoundly after applying electrical stimulation along the direction of the aligned CNTs due to the anisotropic conductivity of the hybrid GelMA-vertically aligned CNT hydrogels. We believe that platform could attract great attention in other biomedical applications, such as biosensing, bioelectronics, and creating functional biomedical devices.

Hydrogels are commonly used as biological scaffolds because of their high water content, biocompatibility, and biodegradability^{1,2}. However, they are typically mechanically weak and electrically non-conductive, limiting their applications in regulating the behavior of electro-active cells, such as skeletal muscle, cardiac, and neural cells³. Therefore, controlling the mechanical and electrical properties of hydrogels is desirable to facilitate the regulation of cell behavior. In particular, anisotropically conductive hydrogels are highly beneficial for the fabrication of functional tissue constructs with the aid of electrical stimulation (ES). Hydrogels with high electrical conductivity and robust mechanical properties have other important applications, for example, in biosensing^{4,5}, in the development of hybrid three-dimensional (3D) electronics-tissue materials^{6,7}, and as bioactuators⁸.

Nanomaterials have been widely used to improve the electrical conductivity and mechanical properties of hydrogels⁹. For example, gold nanostructures have been successfully used to increase the electrical conductivity of alginate hydrogels^{3,10}. The resulting hydrogels exhibited higher performance to electrically stimulate cardiomyo-



cytes and neural cells compared with pristine hydrogels. We recently reported the use of carbon nanotubes (CNTs) to effectively reinforce methacrylated gelatin (GelMA) hydrogels and to generate 3D hybrid GelMA-CNT hydrogels¹¹. GelMA is a photopolymerizable hydrogel composed of natural gelatin functionalized with methacrylic anhydride¹². The formation of nanofiber web-like structures of CNTs within GelMA hydrogels resulted in hybrid GelMA-CNT hydrogels with enhanced mechanical properties compared with the pure GelMA hydrogels¹¹. Despite the unique electrical properties of CNTs, few published studies have reported the tuning of electrical properties of hydrogels using CNTs. Most of the unique properties of CNTs are exerted in the direction of the tube axis¹³. Therefore, the anisotropic electrical and mechanical properties of hybrid hydrogel-CNT systems can be controlled by aligning the CNTs within the hydrogels along their tube axes. Based on this, we propose the use of dielectrophoresis (DEP) as an efficient tool to vertically align CNTs within GelMA hydrogels. DEP is a powerful technique to manipulate particles in a medium based on their responses to an AC electric field, which induces a charge polarization within the particles and the surrounding medium^{14,15}. Due to its low ion concentration and viscosity, GelMA hydrogels provide a suitable milieu for the dielectrophoretic alignment of CNTs. In our previous work, CNTs were horizontally micropatterned inside GelMA hydrogels using DEP¹⁶. It was shown that horizontally aligned CNTs within hybrid GelMA hydrogels were aligned through their axial direction due to DEP forces and formed cylindrically long CNT bundles within GelMA hydrogels. Therefore, cells seeded on these hydrogels could only attach to and sense CNTs in their radial direction¹⁶. In other words, the cells could sense the sides of the CNTs but not the head or tail end groups, which is somehow limiting as CNTs exhibit their unique mechanical and electrical properties in their axial direction¹⁷. In addition, it was not possible to provide local ES for cells seeded on GelMA gels containing horizontally aligned CNTs.

Finally, the interconnected network of horizontally aligned CNTs inside GelMA hydrogels generated a situation in which the electrical current of the underlying electrodes could ‘short circuit’ to a neighboring electrode without approaching cells that were seeded on top of the hydrogels¹⁶. To address these limitations, we changed the direction of the alignment of CNTs within GelMA hydrogels to vertical.

In this paper, we used DEP to vertically align CNTs within GelMA hydrogels. The anisotropic electrical conductivity and mechanical features of the hybrid GelMA hydrogels containing vertically aligned CNTs were evaluated and compared with those of pristine GelMA, hybrid GelMA-randomly dispersed CNT, and GelMA-horizontally aligned CNT hydrogels. To demonstrate the utility of these novel hydrogels, the GelMA-vertically aligned CNT, GelMA-random CNT, and GelMA-horizontally aligned CNT hydrogels were used to fabricate muscle myofibers, which were then characterized in terms of the expression of myogenic genes and proteins, particularly after applying ES along the direction of the aligned CNTs.

Results

To prepare hybrid GelMA-CNT prepolymer for DEP experiment, CNTs were initially functionalized with carboxyl groups to render them water-soluble and then dispersed in a solution containing GelMA. In this mixture, CNTs were stabilized with a thin layer of GelMA polymer, as described in our previous work¹¹. Atomic force microscopy (AFM) measurements showed that pristine CNTs had the thickness 9 ± 8 nm, while the thickness of CNTs coated with the GelMA was found to be 25 ± 12 nm. These results were also confirmed by transmission electron microscopy (TEM) pictures¹¹. DEP was then used to vertically align the CNTs within the GelMA mixture, as shown in Fig. 1. The CNTs were successfully aligned vertically within the GelMA mixture by the application of an AC electric field (2 MHz and 20 V) (see the Supporting Information, Movie S1).

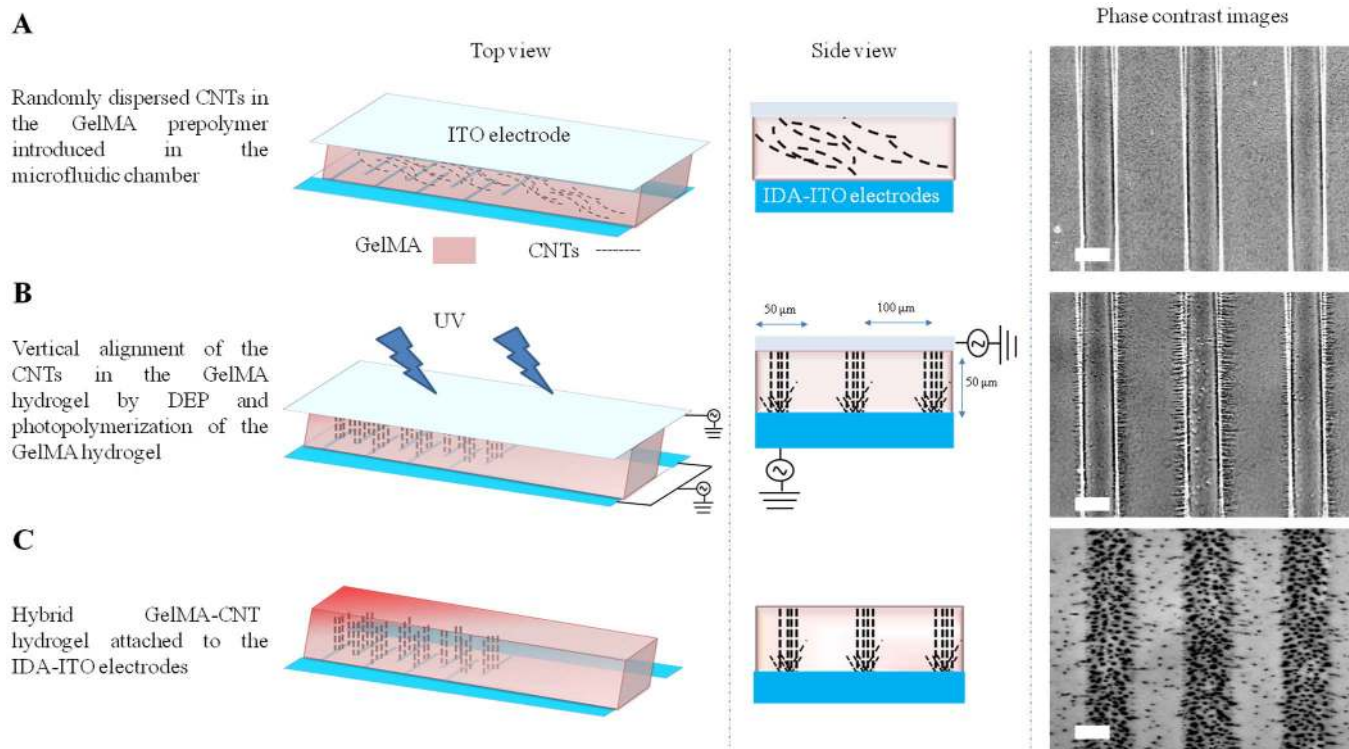


Figure 1 | DEP mediated vertical alignment of CNTs within GelMA hydrogels. (A) Randomly dispersed CNTs within GelMA prepolymer were introduced into a 50- μ m-tall microfabricated chamber. (B) The CNTs in the GelMA prepolymer were vertically aligned on the IDA-ITO electrodes using DEP (voltage 20 V and frequency 2 MHz). The GelMA was then crosslinked by applying UV light for 150 s. (C) The GelMA gel containing vertically aligned CNTs was detached from the glass slide and retained on the IDA-ITO electrodes. Scale bars, 50 μ m.



The alignment of CNTs using the DEP approach was rapid, requiring less than one minute. The AC electric fields appeared to induce dipole moments within the CNTs and forced them to align in the direction of the electric field.

The proposed approach to align CNTs within hydrogels is versatile and can create any desired arrangement of micropatterned CNTs within hydrogels. Any desired micropatterned CNTs in hydrogels can be created by using one corresponding micropatterned electrode in the setup of DEP system. In this paper, CNTs within GelMA hydrogels were also vertically aligned between a top ITO electrode and a bottom interdigitated array of ITO (IDA-ITO) electrodes as shown in Fig. 1 (Supporting Information, Movie S2). Therefore, the CNTs were vertically aligned on the micropatterned ITO electrodes (*i.e.*, IDA-ITO electrodes). The DEP forces disappear when the AC

electric field is switched off. The Supporting Information (Movies S3 and S4) demonstrates how dielectrophoretically aligned CNTs within GelMA hydrogels lose their alignment as the DEP forces disappear. Therefore, a stabilization step is required after applying the DEP forces to preserve the alignment of the CNTs in the absence of the AC electric field. Here, the immobilization step was performed in a rapid and non-destructive manner by crosslinking the GelMA hydrogel with UV light (Fig. 1).

We prepared pristine GelMA hydrogels and hybrid GelMA hydrogels containing vertically aligned, random, and horizontally aligned CNTs with CNT concentrations of 0.5 and 1 mg/mL. The electrical conductivities of these hydrogels were then measured through ITO electrodes to obtain accurate and reproducible conductivity values. As shown in Figs. 2 and S1, the DC electrical conduc-

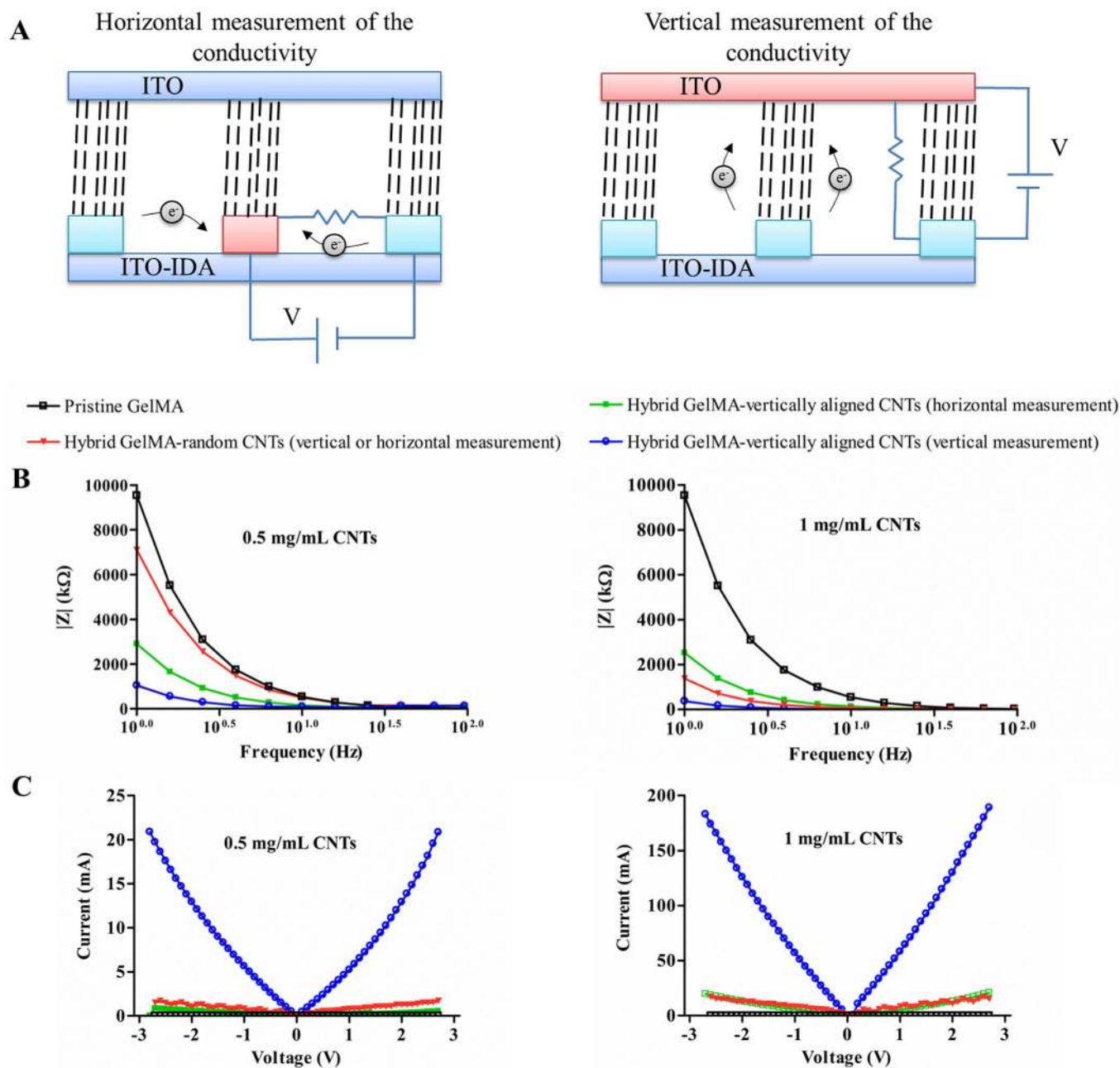


Figure 2 | Anisotropic conductivity of pristine GelMA and hybrid GelMA-CNT gels containing different concentrations of CNTs. (A) Schematic of the systems used for horizontal and vertical measurements of electrical conductivity for hybrid GelMA-vertically aligned CNT hydrogels. (B) Impedance measurements of pristine GelMA and hybrid gels loaded with 0.5 and 1 mg/mL CNTs. The perturbation amplitude was 25 mV. (C) I-V curves for pristine GelMA and GelMA hydrogels containing vertically aligned and random CNTs.



tivity dramatically increased as a function of the CNT concentration. Most importantly, the conductivity of hybrid GelMA-aligned CNT hydrogels for both vertical and horizontal CNT alignment along with CNT alignment was higher than that perpendicular to CNT alignment. For instance, when we applied 2.7 V to the hybrid GelMA-0.5 mg/mL vertically aligned CNT hydrogel, the measured currents were 20.86 and 0.53 mA along with CNT alignment and perpendicular to CNT alignment, respectively. However, the hybrid GelMA-random CNT hydrogels exhibited no anisotropic conductivity. The concept of anisotropic conductivity here refers to a significantly higher electrical conductivity of underlying hydrogels either in the vertical or horizontal measurement of conductivity as schematized in Figs. 2-A and S1-A. The anisotropic conductivity of the hybrid GelMA-aligned CNT hydrogels is primarily due to the generation of an interlinked network of CNTs that enables the propagation of the electrical current. We observed a similar trend in the impedance of the hydrogels (Figs. 2 and S1). For example, the measured impedances of the hybrid GelMA-1 mg/mL vertically aligned CNT hydrogel at the frequency 6.31 Hz were 2096.84 and 22654.64 k Ω along with CNT alignment and perpendicular to CNT alignment, respectively. Impedance spectra were acquired for GelMA and hybrid GelMA-CNT hydrogels over a frequency range from 1 to 100 Hz with a perturbation amplitude of 25 mV.

We also used a micromechanical mapping approach to measure the mechanical properties of GelMA and nanostructured hybrid GelMA-CNT gels. As shown in Fig. 3, the Young's modulus of the pristine GelMA was 12.5 ± 0.1 kPa, consistent with our previously reported value derived from conventional stress-strain measurements¹². As CNTs were added to the GelMA hydrogel, the Young's modulus, as measured by nanoindentation method applied vertically to the hydrogel, increased (Fig. 3-D). However, this increase was more profound for the hybrid GelMA-vertically aligned CNT hydrogels than for the hybrid GelMA-random CNT gels. The Young's modulus values measured for the hybrid GelMA-0.1 mg/mL aligned CNT gel and the GelMA-0.1 mg/mL random CNT gel were 50.4 ± 3.8 and 20.3 ± 1.4 kPa, respectively. The increase in the Young's modulus of the hybrid GelMA-CNT hydrogels compared with the pristine GelMA hydrogel was due to the reinforcing effect of the CNTs within the hydrogels. In this evaluation, the AFM tip vertically tapped the samples along the direction of the aligned CNTs. Therefore, there was an increase in the Young's modulus of the hybrid GelMA-aligned CNT gels relative to that of the hybrid GelMA-random CNT gels. This result is consistent with a previous report that CNTs exhibit their unique mechanical properties in their axial direction¹⁷.

The Young's modulus of GelMA-horizontally aligned CNT was measured to be 23.4 ± 1.7 kPa¹⁶, which is lower than that of GelMA-vertically aligned CNTs at the same CNT concentration (0.3 mg/mL) (48.5 ± 2.3 kPa). This result is in agreement with the previous work that CNTs show their high and unique mechanical properties in their axial direction rather than radial direction¹⁷. As a result, there is no need to increase the mechanical properties of hybrid GelMA-CNT hydrogels by increasing the CNT concentration as this can be achieved by vertically aligning CNTs inside GelMA-CNT hydrogels using the DEP technique. Minimizing the use of CNTs in hybrid hydrogel-CNT materials is always beneficial as to preserve the desired biological properties of the hydrogel materials for biomedical applications.

Interestingly, the Young's modulus of the hybrid GelMA-aligned CNT gels at a CNT concentration of 1 mg/mL was lower than that of hybrid GelMA-aligned CNT gels made using lower CNT concentrations. This may be due to higher UV absorption at higher concentrations, which resulted in a lower degree of crosslinking and as a result were softer. In agreement with this result, we recently demonstrated that the UV absorption of hybrid GelMA-CNT gels is increased upon increasing the CNT concentration¹¹. The force-deformation curves are also shown (first images from the right: Fig. 3-A, 3-B, and 3-C),

taking into consideration one representative point of the corresponding Young's modulus maps. Note that the direction of hydrogel deformation was vertical to the gels. The Young's modulus maps were calculated by the Derjaguin, Muller, and Toporov (DMT) fitting model¹⁸ using the force-deformation plots.

We further evaluated the performance of the hybrid GelMA-vertically aligned CNT, GelMA-random CNT, and GelMA-horizontally aligned CNT hydrogels with a concentration of 0.3 mg/mL in the fabrication of C2C12 muscle myofibers. We previously showed that CNTs had no detectable adverse effect on the viability of C2C12 myoblasts, and more than 95% of myoblasts remained viable on both pristine GelMA and hybrid GelMA-CNT hydrogels after 3 days of culture. In addition, the level of muscle cell proliferation was similar in both hydrogel systems¹⁶. Here, C2C12 myoblasts were randomly cultured on hybrid GelMA-vertically aligned CNT, GelMA-random CNT, and GelMA-horizontally aligned CNT hydrogels. The reason for this cell culture method was to provide a suitable substrate for the cells to sense the vertically aligned CNTs in their axial direction. Therefore, there was no preferential direction for the cell alignment. After 1 day of culture, myoblast differentiation was induced by switching to a differentiation medium. During the differentiation period, the cells expressed myosin heavy chain protein and fused together to form C2C12 myotubes¹⁹. The muscle cells were subjected to ES (voltage, 8 V; frequency, 1 Hz; duration, 10 ms) for 2 continuous days beginning on day 8 of culture. C2C12 myotubes cultured in the absence of ES were used as control samples. It is well known that the calcineurin pathway is responsible for tonic and low frequency nerve stimulation in body leading to fast-to-slow muscle myofiber transformation²⁰. Calcineurin is a Ca²⁺/calmodulin-dependent protein phosphatase that regulates nuclear translocation of the NFAT (nuclear factor of activated T cells) transcription factor and activation of target genes. The employed ES protocol here mimics tonic and low frequency nerve stimulation for native muscles in body²¹. As a result of such stimulation, anabolic processes occur that are required for the expression of proteins and genes related to myofiber formation. Muscle cell proliferation may be also involved during stimulation process leading to enlarge muscle myofibers²². Therefore, myotube analysis and gene expression profiles are good measures to evaluate the effect of ES on muscle myofibers.

The myotube analysis was performed using two groups of electrically stimulated myotubes and control samples cultured on hybrid GelMA-vertically aligned CNT, GelMA-random CNT, and GelMA-horizontally aligned CNT hydrogels on day 10 of culture (Fig. 4). The C2C12 myoblasts on the hybrid GelMA-aligned CNT hydrogels exhibited enhanced differentiation compared with the cells on the GelMA-random CNT and GelMA-horizontally aligned CNT hydrogels even when no electric field was applied. The average myotube length for the C2C12 myotubes on the hybrid GelMA-vertically aligned CNT hydrogels was significantly longer than that on the GelMA-random CNT hydrogels (59.41 ± 20.91 μ m and 142.03 ± 57.07 μ m, respectively). The myotube coverage area for the C2C12 myotubes on the hybrid GelMA-vertically aligned CNT hydrogels was significantly higher than that on the GelMA-horizontally aligned CNT hydrogels (12.34 ± 2.05 and $16 \pm 1\%$, respectively). This observed difference may be due to the differences in the mechanical properties of the two substrates. It is expected that the hybrid GelMA-vertically aligned CNT hydrogels would provide more anchoring sites for cellular adhesion and differentiation than the GelMA-random CNT and GelMA-horizontally aligned CNT hydrogels. In our previous work²³, we showed that the C2C12 muscle cells had more extended pseudopodia and branched filopodia on the hybrid CNT-fibronectin (Fn) surfaces compared with those on the pristine Fn surfaces confirming the significant mechanotaxic effect of CNTs to create anchoring sites for the cells. Both the average myotube length and coverage area values for the C2C12 myotubes that were electrically stimulated on the hybrid GelMA-vertically aligned

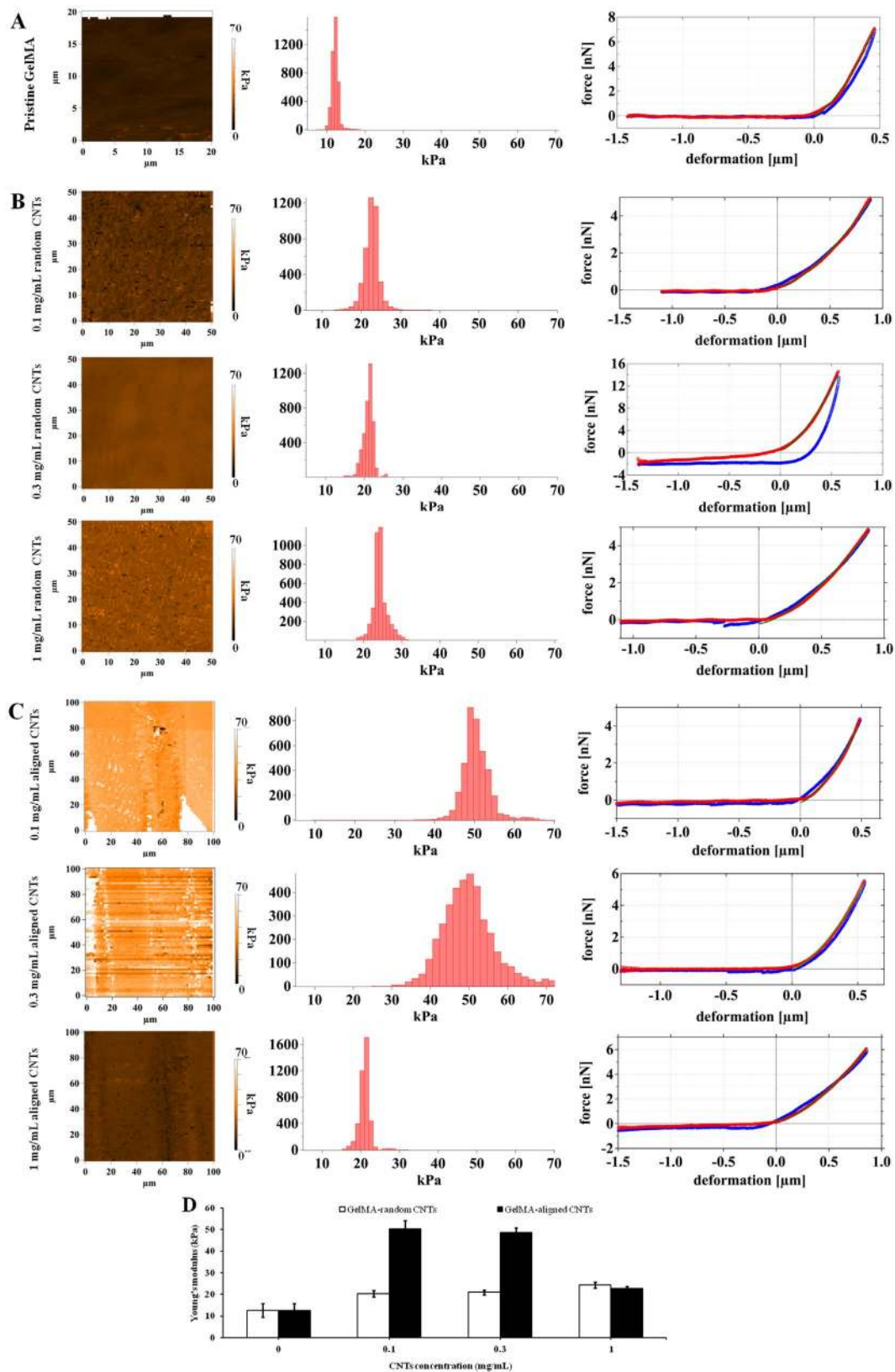


Figure 3 | Mechanical properties of pristine GelMA and hybrid GelMA-CNT hydrogels containing different concentrations of CNTs (0.1, 0.3, and 1 mg/mL), as measured by AFM. (A) Young's modulus map, Young's modulus distribution, and force deformation curves for pristine 5% GelMA hydrogels (left to right, respectively). The red curve represents the force deformation curve as the AFM cantilever approached the surface, and the blue curve is the force deformation curve produced when the cantilever left the surface. The green line was calculated according to the DMT theory. (B) Young's modulus map, Young's modulus distribution, and force deformation curves for hybrid GelMA-random CNT hydrogels (left to right, respectively). (C) Young's modulus map, Young's modulus distribution, and force deformation curves for hybrid GelMA-vertically aligned CNT hydrogels (left to right, respectively). Data in part (D) are presented as mean \pm standard deviation obtained from at least 5 AFM pictures with 4096 independent data points in each.

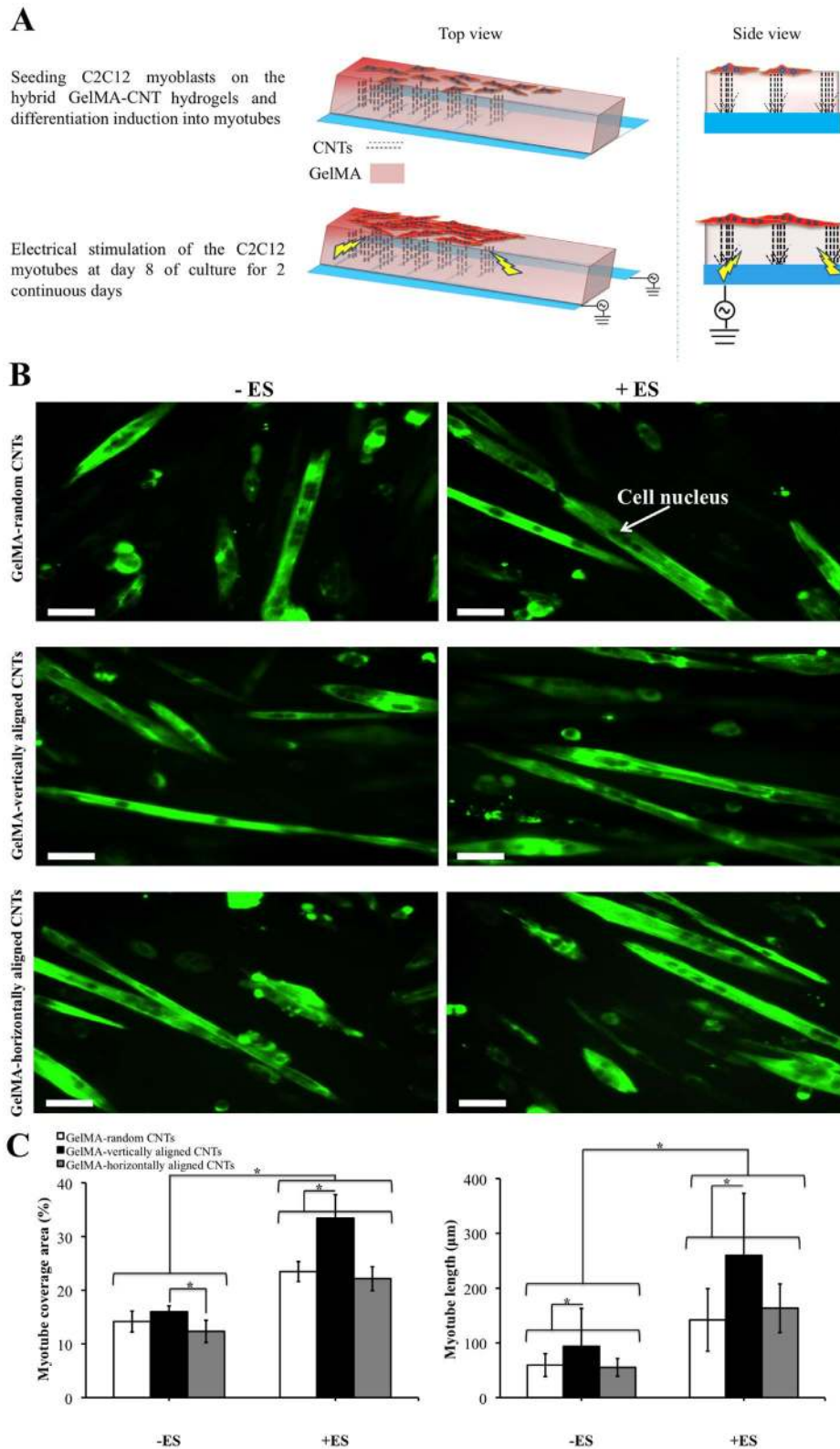


Figure 4 | Differentiation of C2C12 myoblasts on GelMA-0.3 mg/mL CNT hydrogels and characterization of the C2C12 myotubes obtained under ES. (A) Schematic representation of the procedure used to produce and electrically stimulate C2C12 myotubes. (B) Immunostaining of the fast skeletal myosin heavy chain in the C2C12 myotubes fabricated on hybrid GelMA-random CNT, GelMA-vertically aligned CNT, and GelMA-horizontally aligned CNT hydrogels with and without ES application (indicated as +ES and -ES, respectively) on day 10 of culture. Cell nuclei within the C2C12 myotubes were obvious after the staining procedure. The ES parameters were as follows: a voltage of 8 V, a frequency of 1 Hz, and a duration of 10 ms. The scale bars represent 50 μm . (C) Quantification of the myotube coverage area and myotube length of the C2C12 myotubes fabricated on hybrid GelMA-random CNT, GelMA-vertically aligned CNT, and GelMA-horizontally aligned CNT hydrogels with and without ES on day 10 of culture. Data in part (C) are presented as mean \pm standard deviation obtained from at least 40 myotubes of 2 independent experiments. Asterisks indicate significant differences between samples ($*p < 0.05$).



CNT hydrogels ($259.89 \pm 113.05 \mu\text{m}$ and $33 \pm 4\%$, respectively) were significantly greater than those of the unstimulated myotubes ($93.83 \pm 68.84 \mu\text{m}$ and $16 \pm 1\%$, respectively). Although the same trend was observed when comparing the electrically stimulated C2C12 myotubes with unstimulated myotubes cultured on the GelMA-random CNT and GelMA-horizontally aligned CNT hydrogels, the ES had a more profound effect on the muscle myofibers cultured on the hybrid GelMA-aligned CNT hydrogels. In particular, the average myotube length was increased 277% upon applying the ES for the C2C12 myotubes cultured on the hybrid GelMA-aligned CNT hydrogels, while this increase was 239% for those cells on the hybrid GelMA-random CNT hydrogels. The average coverage area was also increased 209% upon applying the ES for the C2C12 myotubes cultured on the hybrid GelMA-aligned CNT hydrogels, while this parameter was increased 165.65 and 180% for the muscle cells cultured on the hybrid GelMA-random CNT and GelMA-horizontally aligned CNT hydrogels, respectively. The enhanced effect is likely due to the vertical alignment of the CNTs in the hybrid GelMA-aligned CNT hydrogels, which increased the efficiency of the ES along the direction of the CNT alignment for muscle cells on the top of hydrogels in the hybrid GelMA-vertically aligned CNT hydrogels compared with that in the GelMA-random CNT and GelMA-horizontally aligned CNT hydrogels. Even though GelMA-horizontally aligned CNT hydrogels also demonstrated the anisotropic electrical conductivity, the preferred direction of electric field within these hydrogels was not favorable for the muscle cells cultured on the top of these hydrogels. In other words, the interconnected network of horizontally aligned CNTs inside GelMA hydrogels provided a short circuit for the electrical current to pass through neighboring electrodes without approaching the cells on the top of hydrogels. Therefore, GelMA-horizontally aligned CNT hydrogels were less efficient in fabricating functional muscle myofibers compared with GelMA-vertically aligned CNT hydrogels.

Fig. 5 shows the gene expression values of fabricated muscle myofibers cultured on hybrid GelMA-vertically aligned CNT, GelMA-random CNT and GelMA-horizontally aligned CNT hydrogels with or without ES application. Myogenin and MRF4 interact with the muscle protein LIM during muscle maturation and are highly expressed in mature adult skeletal muscles²⁴. Sarcomeric actin, α -actinin, and myosin heavy chain isoform IId/x (MHCIId/x) are contraction-related genes that are expressed as a result of sarcomeric development within the muscles. Importantly, the ES substantially promoted myoblast differentiation, and this effect was more profound for myofibers cultured on hybrid GelMA-vertically aligned CNT hydrogels than for those cultured on hybrid GelMA-random CNT and GelMA-horizontally aligned CNT hydrogels. Again, this difference is primarily attributed to the anisotropic conductivity along the direction of the ES for the hybrid GelMA-vertically aligned CNT hydrogels.

Discussion

In this work, DEP method was used to vertically align CNTs within GelMA hydrogels in a robust, simple, and rapid manner. There are a number of other methods for aligning CNTs on or in biomaterials. For example, Sung *et al.* used an electrospinning method to align CNTs within poly(methyl methacrylate)²⁵. However, as the concentration of CNTs was increased to 5 wt%, the alignment of the CNTs became irregular due to CNT aggregation during the electrospinning process. Generally, the electrospinning method for aligning CNTs is not highly efficient, likely due to a relaxation step after the formation of the electrospun fibers²⁶ and the highly tangled nature of the electrospun hybrid biomaterial-CNTs, which leads to bent and twisted CNTs and aggregate formation^{27,28}. Another approach to obtain aligned CNTs within a biomaterial is to apply mechanical strain to hybrid biomaterial-CNT systems. Voge *et al.* employed this method to align CNTs within collagen-fibrin hydrogels²⁹. They also showed

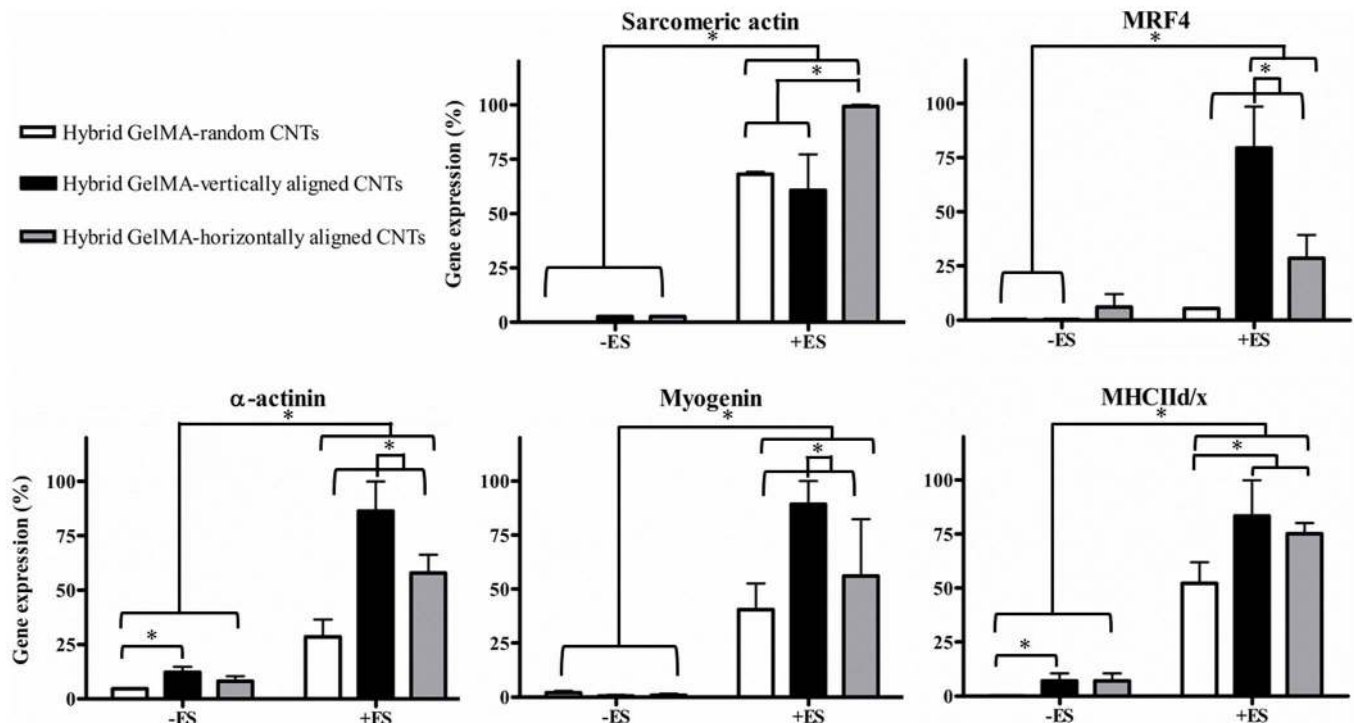


Figure 5 | Gene expression analysis of C2C12 myotubes fabricated on GelMA-0.3 mg/mL CNT hydrogels subjected to ES. Expression levels of sarcomeric actin, MRF4, α -actinin, myogenin, and MHCIId/x in fabricated muscle myofibers grown on GelMA hydrogels containing random CNTs, vertically aligned CNTs, and horizontally aligned CNTs. The ES was applied on day 8 of culture with a voltage of 8 V, a frequency of 1 Hz, and a duration of 10 ms continuously for 2 consecutive days. The expression levels of the genes were normalized based on the level of the internal reference gene GAPDH. Data are presented as mean \pm standard deviation obtained from at least 8 measurements of 2 independent experiments. Asterisks indicate significant differences between samples (* $p < 0.05$).



that hydrogels with anisotropic CNTs had higher conductivities than hydrogels containing randomly dispersed CNTs. However, this technique requires several hours and is not suitable for aligning CNTs within a soft biomaterial. CNTs were also aligned using a simple spinning method³⁰. However, this technique can be used to align CNTs in the radial direction only. Other vertically aligned nanostructures, such as vertically aligned carbon nanofibers (CNFs), have also been fabricated for biomedical applications³¹. CNFs are multi-walled graphene structures that are stacked on top of each other³². These vertically aligned structures have been widely used as neuronal interfaces, gene delivery arrays, and biosensors^{33,34}. Generally, these nanostructures are synthesized *via* plasma-enhanced chemical vapor deposition and are aligned perpendicular to a conductive substrate. This process is long and requires several steps that involve chemical reactions and must take place under high vacuum. In contrast, our proposed DEP approach can produce vertically aligned CNT nanostructures in a facile and rapid manner without using toxic chemicals and complicated experimental setups.

It was demonstrated that GelMA gels containing either vertically or horizontally aligned CNTs had anisotropic electrical conductivity. However, as shown previously, the anisotropic conductivity of GelMA-vertically aligned CNT hydrogels provides more efficient ES through the electrodes patterned below the hydrogel to cells cultured on top of these gels compared with GelMA-random CNT and more importantly with GelMA-horizontally aligned CNT hydrogels with the anisotropic electrical conductivity. The latter fact was also confirmed by simulating the applied electric fields to cells on pristine GelMA, GelMA-random CNT, GelMA-horizontally aligned CNT, and GelMA-vertically aligned CNT hydrogels (Fig. 6) and calculating the current densities on the top of gels. The current densities were 0.95, 340, 320, and 700 A/m² on the top of pristine GelMA, GelMA-random CNT, GelMA-horizontally aligned CNT, and GelMA-vertically aligned CNT hydrogels, respectively, with 10 μm thickness. An increase in the hydrogel thickness led to a decrease in the current densities. Interestingly, there was more current density on GelMA-random CNT with 50 μm thickness compared with GelMA-horizontally aligned CNT with the same thickness. The current densities were 0.65, 180, 0.75, and 340 A/m² on the top of pristine GelMA, GelMA-random CNT, GelMA-horizontally aligned CNT, and GelMA-vertically aligned CNT hydrogels. These results are in agreement with the previous report that the electrical conductivity of aligned multi-walled CNTs was 1000 S/m along with the longitudinal axis of nanotubes, while it was reported to be 150 S/m perpendicular to the nanotube axis³⁵. Such hybrid GelMA-vertically aligned CNT hydrogels with the

favorable anisotropic conductivity may attract great attention in various biomedical applications, such as tissue engineering, biosensing and monitoring, and bioelectronics.

The mechanical properties of scaffolds affect cell behaviors and functions, such as cell adhesion, proliferation, and differentiation³⁶. Therefore, hydrogels with tunable mechanical properties are highly desirable. It is possible to enhance the mechanical properties of hydrogels by simply increasing the hydrogel concentration. However, this concentration increase reduces the porosity and interconnectivity of the hydrogels and therefore has adverse effects on hydrogel performance³⁷. For example, we recently demonstrated that enhancing the mechanical properties of GelMA hydrogels by increasing the concentration or the degree of methacrylation reduced cell viability, proliferation, and migration³⁸. Thus, CNTs may be extremely promising as supplementary materials for hydrogels to permit the tuning of their mechanical properties. Due to the extraordinary mechanical properties of CNTs, small amounts of CNTs are sufficient to considerably change the mechanical properties of hybrid hydrogel-CNTs, with minor effects on the beneficial properties of the hydrogels.

We showed that GelMA-vertically aligned CNT hydrogels provides more efficient ES to cells cultured on top of these gels compared with GelMA-randomly dispersed CNT and GelMA-horizontally aligned CNT hydrogels. In a relevant study, Kaji *et al.* cultured C2C12 cells on a poly(dimethylsiloxane) (PDMS) membrane³⁹. The local ES of C2C12 myotubes through holes in the PDMS substrate, which was achieved with the aid of Pt electrodes vertically placed around the membrane, induced the differentiation of the muscle cells compared with unstimulated samples. However, in the present study, we developed a robust and efficient platform to tune the electrical conductivity of hydrogels by altering the alignment and concentration of CNTs, thus allowing for control of the differentiation of the skeletal muscle cells. Controlling the differentiation of skeletal muscle cells is a useful tool for regulating the metabolism and glucose consumption of the corresponding muscle tissues³⁹. The skeletal muscle tissues play a crucial role in maintaining the glucose level in the body, and any abnormality in glucose uptake by skeletal muscle can lead to type 2 diabetes⁴⁰. Therefore, the muscle tissue models with controllable differentiation developed in this study are of great interest for screening drugs to treat type 2 diabetes in a high-throughput manner and to investigate the mechanisms of exercise- and insulin-induced glucose uptake by skeletal muscle tissues. Such engineered tissues could also be less expensive and time consuming than animal experiments and could serve as a step in the transition toward personalized medicine. Hydrogels with tunable electrical

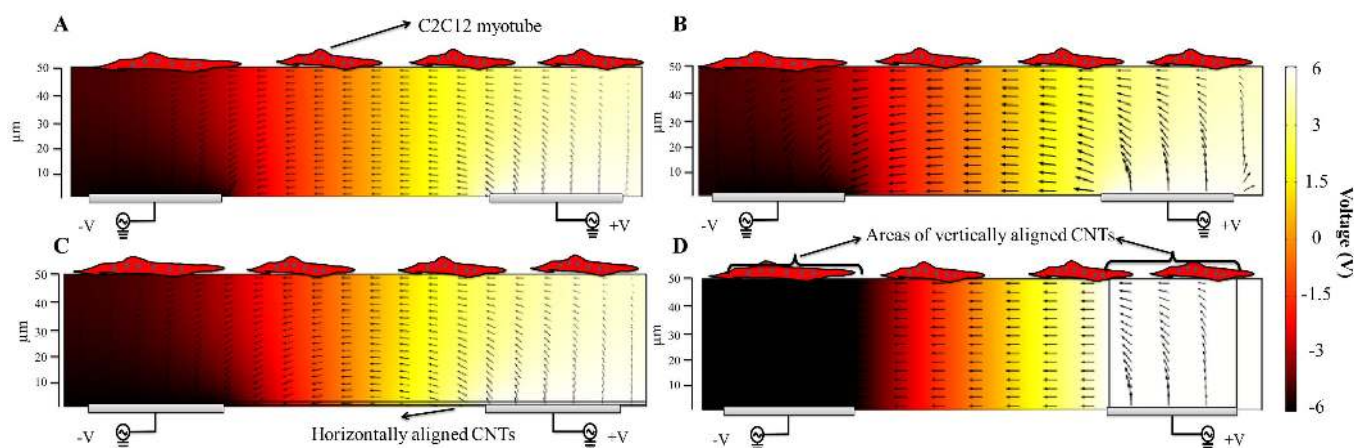


Figure 6 | Simulation of applied electric fields to muscle cells cultured on hydrogels. Cross-sectional views of the numerically calculated electric fields (V/m) applied to muscle cells cultured on (A) pristine GelMA, (B) GelMA-random CNT, (C) GelMA-horizontally aligned CNT, and (D) GelMA-vertically aligned CNT hydrogels. Arrows show the current density (A/m²). Bottom grey bars show the ITO electrodes.



conductivity are also promising candidates for the control of the contraction and therefore the movement of fabricated muscle tissues in bioactuators or biomedical devices.

In summary, we fabricated GelMA hydrogels with tunable electrical conductivity based on CNT alignment and the CNT concentration in a robust, simple, and rapid manner. The GelMA-aligned CNT hydrogels exhibited anisotropic electrical conductivity, which was not observed in the pristine GelMA hydrogels or the GelMA hydrogels containing randomly distributed CNTs. C2C12 myoblasts grown on the hybrid GelMA-vertically aligned CNT hydrogels yielded more functional myofibers, particularly after applying electrical stimulation in the direction of the aligned CNTs, than cells that were cultured on the GelMA hydrogels with randomly distributed and horizontally aligned CNTs. GelMA-CNT hydrogels with tunable electrical properties may be useful in drug screening, in the development of hybrid 3D electronic-tissue materials, and as bioactuators.

Methods

Materials. The materials and suppliers used were as follows: highly pure multi-walled CNTs (Hodogaya Chemical Co., Ltd.); hexamethyldisilazane (Tokyo Ohka Kogyo Co., Ltd., Kanagawa, Japan); developer (MF CD-26) and positive g-line photoresist (S1818) (Shipley Far East Ltd., Tokyo, Japan); methacrylic anhydride, 3-(trimethoxysilyl)propyl methacrylate (TMSPMA), gelatin type A made from porcine skin, and penicillin/streptomycin (P/S) (Sigma-Aldrich Chemical Co., USA); 2-hydroxy-1-[4-(2-hydroxyethoxy)phenyl]-2-methyl-1-propanone (Irgacure 2959) (Ciba Chemicals, Osaka, Japan); fetal bovine serum (FBS) (Bioserum, Japan); and Dulbecco's modified Eagle medium (DMEM), trypsin/EDTA, MEM essential amino acids, MEM nonessential amino acids, and insulin (Invitrogen, USA).

CNT functionalization. Pristine, highly graphitized CNTs synthesized in a catalytic chemical vapor deposition process are hydrophobic in nature. To make them hydrophilic, their surfaces were functionalized by a controlled acid treatment process as described previously^{41,42}. Briefly, CNTs were refluxed in 120 mL of a 3:1 v/v ratio of 98% H₂SO₄ and 68% HNO₃ for 20 min at 110°C. The treated CNTs were then thoroughly washed with ultrapure water on a 1.2 μm membrane and dispersed in ultrapure water (~1 mg/mL) by probe sonication at room temperature for several hours. The resulting CNTs were hydrophilic (zeta potential ~-40 mV in an aqueous solution with a natural pH of ~4.1) and had a high degree of crystallinity, as demonstrated by Raman spectroscopy, scanning electron microscopy, and TEM in our previous works^{41,42}.

GelMA hydrogel synthesis and preparation of its prepolymer. The GelMA prepolymer was synthesized as described elsewhere⁴³. In brief, 12 mL of methacrylic anhydride was added to 6 g of gelatin in phosphate-buffered saline (PBS) for 1 hr at 50°C, resulting in a high degree of methacrylation (~80%) of the gelatin. The mixture was dialyzed with a 12–14 kDa dialysis membrane against distilled water for one week at 40°C and then lyophilized for one week. The GelMA hydrogel was stored at -20°C until use. The GelMA hydrogel (10% [w/v]) was dissolved in MilliQ water with 1% (w/v) photoinitiator (Irgacure 2959), stored at 60°C to complete the GelMA synthesis process, and then used in experiments.

Design and fabrication of the IDA-ITO electrodes. The effective electrode dimensions were 8 × 12 mm². The band electrode was 50 μm in width, and the distance between two neighboring band electrodes was 100 μm (Fig. 1). The band electrode was fabricated on a glass slide (thickness, 1 mm; Matsunami Co., Japan) by conventional photolithography and chemical etching using an etchant solution (HCl:H₂O:HNO₃:4:2:1 by volume) for 15 min under ultrasonication.

Fabrication of aligned CNTs within GelMA hydrogels. The IDA-ITO electrodes were treated with plasma oxygen and methacrylated with TMSPMA under vacuum for 1 hr. Polyethylene terephthalate film spacers (thickness, 10 μm) were used to create a chamber between the ITO electrode and the IDA-ITO electrodes, as shown in Fig. 1. GelMA prepolymer (5%) was mixed with different concentrations of CNTs and placed in an ultrasonic bath for 15 min. The solutions were maintained at 37°C to ensure that the liquid state was maintained before and during the dielectrophoretic patterning of the CNTs within the GelMA hydrogel. To create the gels, 20 μL of the hydrogel-CNT mixture was pipetted between the ITO electrode and the IDA-ITO electrodes (top and bottom electrodes in Fig. 1, respectively) to fill the chamber (8 × 12 × 0.01 mm³). A sinusoidal AC signal (frequency 2 MHz and voltage 20 V) was applied to the IDA-ITO electrodes, and another independent AC signal with an opposite phase was applied to the top ITO electrode to create a nonuniform electric field and vertically align the CNTs. To obtain horizontally aligned CNTs within GelMA hydrogels, a sinusoidal AC signal (frequency 2 MHz and voltage 20 V) was applied to one electrode band of IDA-ITO electrodes, and another independent AC signal with an opposite phase was applied to another electrode band of IDA-ITO electrodes to create a nonuniform electric field. After 1 min, the GelMA prepolymer was polymerized with 7 mW/cm² UV light (Hayashi UL-410UV-1; Hayashi

Electronic Shenzhen Co., Ltd., Japan) for 150 s. After polymerization, the hybrid hydrogels were detached from the DEP device and used in further experiments.

Mechanical properties of GelMA and hybrid GelMA-CNT hydrogels. The mechanical properties of the GelMA and GelMA-CNT hydrogels were investigated using a nanomechanical mapping technique using AFM based on force-distance curve measurements, as described in our previous studies^{44,45}. A Multimode 8 AFM (Bruker Co., USA) equipped with a liquid chamber was used. The AFM cantilever was equipped with a colloidal probe with a 1.0 μm radius (PT.GS, Novascan Technologies, USA) to measure the low elastic modulus values of the underlying hydrogels. The spring constant of the cantilever was measured using the thermal noise method⁴⁶. The force-deformation plots (Fig. 3) were measured by the AFM method. They were then used to calculate the Young's modulus values of hydrogels by the DMT fitting model. The DMT model⁴⁸ describes a kind of contact mechanics between an indenting probe and an elastic surface in which adhesion forces are taken into account and the probe-sample geometry is constrained to be the Hertzian contact. This model has widely been used to analyze AFM-based nano-indentation results.

Electrical properties of GelMA and hybrid GelMA-CNT hydrogels. The current-voltage (I-V) characterization of the hydrogels at room temperature was performed using a two-probe station (HiSOL, Inc., model H19S00556) connected to an I-V analyzer unit (Agilent, model B1500A). The currents between the probes were automatically measured during the automated voltage sweep (-3 to 3 V; 0.1 V steps). Triaxial cables were used in the measurement setup to reduce noise and thus precisely measure currents of approximately 10⁻¹⁰ A. Note that there was no need to use external electrodes for the measurements because the IDA-ITO and top ITO electrodes were used as the electrodes.

Electrochemical impedance spectroscopy (EIS) measurements were collected using a CompactStat potentiostat (CompactStat; Ivium Technologies, Netherlands) controlled by a computer equipped with IviumSoft software. EIS spectra were acquired for the GelMA and hybrid GelMA-CNT hydrogels over a frequency range from 1 to 100 Hz with a perturbation amplitude of 25 mV.

Cell culture. C2C12 myoblasts (American Type Culture Collection, USA) were cultured in DMEM supplemented with 10% FBS and 1% P/S. The C2C12 myoblasts were trypsinized using 0.25% trypsin/0.1% EDTA when they reached 70–80% confluence. The cells were maintained in a cell culture incubator (Sanyo, Japan) with 5% CO₂ at 37°C.

Culture of C2C12 myoblasts on GelMA and hybrid GelMA-CNT hydrogels. For cell culture on GelMA and hybrid GelMA-CNT hydrogels, C2C12 myoblasts were trypsinized, counted, and resuspended in DMEM at a density of 1 × 10⁵ cells/mL. Then, 100 μL of the cell suspension was pipetted onto each hydrogel, and the samples were incubated at 37°C for 30 min to allow cell seeding. After seeding, additional medium was added for extended cell culture. After 1 day of culture, the culture medium was replaced with differentiation medium (DMEM with 2% horse serum, 1 nM insulin, and 1% P/S). The differentiation medium was replenished every 2 days during the culture period.

Immunostaining and characterization of C2C12 myotubes. C2C12 myotubes were immunostained as detailed elsewhere^{47,48}. In brief, the C2C12 myotubes were fixed with 3–4% paraformaldehyde for 12 min, followed by a wash with PBS. The permeabilization step was performed with 0.3% Triton X-100 for 5 min at ambient temperature. Then, the cells were exposed to 5% bovine serum albumin dissolved in PBS for 15 min. A primary mouse monoclonal IgG antibody (ab-7784, Abcam®, Japan) against fast skeletal myosin was added to the samples at a dilution of 1:1000 in PBS, and the samples were incubated at 4°C for 24 hr. The samples were then washed three times with PBS, treated with a goat anti-mouse AlexaFluor® 488 antibody (Invitrogen, USA) at a dilution of 1:1000 in PBS, and incubated at 37°C for 1 hr. The C2C12 myotubes were imaged with a fluorescence microscope. The average myotube length was quantified using the AxioVision Rel. 4.8 software package, and the myotube coverage area was computed with the NIH ImageJ software package.

Electrical stimulation of the engineered muscle myofibers. On day 8 of culture, C2C12 myotubes were electrically stimulated through the IDA-ITO electrodes on the bottom of engineered muscle tissues. As reported in our previous studies, this device is more efficient for stimulating engineered tissues than conventional electrical stimulators^{49–51}. For the ES of muscle myofibers, the differentiation medium was replaced with stimulation medium composed of DMEM with 2% horse serum, 1 nM insulin, 2% MEM essential amino acids, 1% MEM nonessential amino acids, and 1% P/S. Electrical pulses were applied to the muscle myofibers using a waveform generator (WF 1946B Multifunction Synthesizer; NF Co., Japan) with a specified regime (voltage, 8 V; frequency, 1 Hz; duration, 10 ms) continuously for 2 consecutive days. The generated electric current was confirmed using an oscilloscope (WaveSurfer 424; LeCroy Co., Japan). During ES of the muscle myofibers, the stimulation medium was replenished daily to decrease the negative effects of accumulated charge in the medium.

RNA extraction and complementary DNA (cDNA) synthesis. Muscle myofibers were fixed using liquid nitrogen and thoroughly pulverized with a mortar and pestle. RNA was extracted from the muscle myofibers using β-mercaptoethanol and purified



in accordance with the manufacturer's protocol (RNeasy[®] Micro Kit; Qiagen, Venlo, Netherlands). Up to 3 μg of total RNA was reverse transcribed using the QuantiTect Reverse Transcription kit as recommended by the manufacturer (Qiagen, Venlo, Netherlands). To synthesize cDNA, 12 μL of sample (3 μg of total RNA) was diluted with 14 μL of RNase-free water and 4 μL of gDNA wipeout buffer. The prepared samples were incubated for 2 min at 42°C and then cooled to 4°C. The Quantiscript Reverse Transcriptase and Reverse Transcriptase primer mix were added, and the mixture was incubated for 15 min at 42°C, followed by 3 min at 95°C. The samples were kept at 4°C until used for quantitative PCR (qPCR).

Real-time PCR. All primer sets (*i.e.*, primers for GAPDH, myogenin, MRF4, sarcomeric actin, α -actinin, and MHCIIId/x) were purchased from Operon Biotechnologies (Tokyo, Japan) and validated for qPCR experiments. The primer sequences are 5'-TGCTGTGTCAGGCTGGGTGTG-3'/5'-TCGCTGGGCTGGGTGTAG-3', 5'-CGAAAGGAGGAGACTAAAG-3'/5'-CTGTAGACGCTCAATGTAG-3', 5'-ATGTTAGGTATGGGTGAG-3'/5'-GATCTTCTCCATGTGTC-3', 5'-TCATCTCCGCTTCGCCATTC-3'/5'-CTTCAGCATCCAACATCTTAGG-3', and 5'-GCGACAGACACCTCC-3'/5'-TCCAGCCAGCCAGCGATG-3' for myogenin, MRF4, sarcomeric actin, α -actinin, and MHCIIId/x, respectively⁴⁹. Real-time PCR was performed using the Roche LightCycler 1.5 (Roche, Mannheim, Germany) with 2 μL of cDNA, 2 μL of the appropriate primer set, and 14 μL of LightCycler FastStart DNA Master SYBR Green 1 reaction mix (Roche, Mannheim, Germany). Following an initial denaturation step at 95°C for 10 min, real-time PCR was performed over 45 cycles of 95°C for 10 s, 62°C for 10 s, and 72°C for 20 s, followed by a melting curve analysis. The expression levels of the target genes were normalized against that of the GAPDH gene⁵². The gene expression analysis was repeated at least four times for each sample.

Simulation of electric fields. The distribution of electric fields within the gels (*i.e.*, pristine GelMA, GelMA-random CNT, GelMA-horizontally aligned CNT, and GelMA-vertically aligned CNT hydrogels) was computed using the finite element analysis as implemented in the COMSOL Multiphysics 4.2, Stockholm, Sweden (Fig. 6). The size of bottom ITO electrodes was set to 50 μm . The potential difference and distance between two neighboring ITO electrodes were 6 V and 100 μm , respectively. The height of hydrogels on the top of electrodes was 50 μm . In the case of the hybrid GelMA-horizontally aligned CNT, it was assumed that CNT layer between the ITO electrodes has 0.5 μm thickness. For the hybrid GelMA-vertically aligned CNT hydrogel, the CNT alignment was supposed to be on the top of ITO electrodes. The electrical conductivities of all underlying hydrogels were obtained from the experimental data (see Fig. 2). Viscosity of 5 wt% GelMA hydrogel was set to 0.09 cm^2/s as reported in our previous work⁵³. The current density (A/m^2) was also calculated for the hydrogels with 10 and 50 μm thicknesses.

Statistical analysis. Significant differences were identified using the independent Student's *t*-test for two groups of data using the MINITAB 16.0 statistical software package (Minitab Inc., USA). All data from repeated experiments are reported as the average \pm standard deviation, and *p*-values less than 0.05 were deemed significant.

1. Peppas, N. A., Hilt, J. Z., Khademhosseini, A. & Langer, R. Hydrogels in biology and medicine: From molecular principles to bionanotechnology. *Adv. Mater.* **18**, 1345–60 (2006).
2. Slaughter, B. V., Khurshid, S. S., Fisher, O. Z., Khademhosseini, A. & Peppas, N. A. Hydrogels in regenerative medicine. *Adv. Mater.* **21**, 3307–29 (2009).
3. Dvir, T. *et al.* Nanowired three-dimensional cardiac patches. *Nat. Nano.* **6**, 720–5 (2011).
4. Tian, B. *et al.* Macroporous nanowire nanoelectronic scaffolds for synthetic tissues. *Nat. Mater.* **11**, 986–94 (2012).
5. Xu, L. *et al.* Design and synthesis of diverse functional kinked nanowire structures for nanoelectronic bioprobes. *Nano Lett.* **13**, 746–51 (2013).
6. Schwillie, P. Bottom-up synthetic biology: Engineering in a tinkerer's world. *Science* **333**, 1252–4 (2011).
7. Sapra, K. T. & Bayley, H. Lipid-coated hydrogel shapes as components of electrical circuits and mechanical devices. *Sci. Rep.* **2**, 848 (2012).
8. Shin, S. R. *et al.* Carbon-nanotube-embedded hydrogel sheets for engineering cardiac constructs and bioactuators. *ACS Nano* **7**, 2369–80 (2013).
9. Dvir, T., Timko, B. P., Kohane, D. S. & Langer, R. Nanotechnological strategies for engineering complex tissues. *Nat. Nanotech.* **6**, 13–22 (2011).
10. You, J.-O., Rafat, M., Ye, G. J. C. & Auguste, D. T. Nanoengineering the heart: Conductive scaffolds enhance Connexin 43 expression. *Nano Lett.* **11**, 3643–8 (2011).
11. Shin, S. R. *et al.* Carbon nanotubes reinforced hybrid microgels as scaffold materials for cell encapsulation. *ACS Nano* **6**, 362–72 (2012).
12. Nichol, J. W. *et al.* Cell-laden microengineered gelatin methacrylate hydrogels. *Biomaterials* **31**, 5536–44 (2010).
13. MacDonald, R. A., Voge, C. M., Kariolis, M. & Stegemann, J. P. Carbon nanotubes increase the electrical conductivity of fibroblast-seeded collagen hydrogels. *Acta Biomater.* **4**, 1583–92 (2008).
14. Ramón-Azcón, J. *et al.* Competitive multi-immunosensing of pesticides based on the particle manipulation with negative dielectrophoresis. *Biosens. Bioelectron.* **25**, 1928–33 (2010).

15. Ramón-Azcón, J. *et al.* Detection of pesticide residues using an immunodevice based on negative dielectrophoresis. *Biosens. Bioelectron.* **24**, 1592–7 (2009).
16. Ramón-Azcón, J. *et al.* Dielectrophoretically aligned carbon nanotubes to control electrical and mechanical properties of hydrogels to fabricate contractile muscle myofibers. *Adv. Mater.* **25**, 4028–34 (2013).
17. Estili, M., Kawasaki, A. & Sakka, Y. Highly concentrated 3D macrostructure of individual carbon nanotubes in a ceramic environment. *Adv. Mater.* **24**, 4322–6 (2012).
18. Derjaguin, B. V., Muller, V. M. & Toporov, Y. Effect of contact deformations on the adhesion of particles. *J. Colloid Interf. Sci.* **53**, 314–26 (1975).
19. Andrés, V. & Walsh, K. Myogenin expression, cell cycle withdrawal, and phenotypic differentiation are temporally separable events that precede cell fusion upon myogenesis. *J. Cell Biol.* **132**, 657–66 (1996).
20. McCarthy, J. J. & Esser, K. A. Skeletal Muscle Adaptation to Exercise in Muscle: Fundamental Biology and Mechanisms of Disease. Edited by Hill, J. A., Olson, E. N. & San Diego, C. A: Academic Press, Chapter 64, 911–920.
21. Schiaffino, S. & Serrano, A. Calcineurin signaling and neural control of skeletal muscle fiber type and size. *Trends Pharmacol. Sci.* **23**, 569–75 (2002).
22. Bickel, C. S. *et al.* Time course of molecular responses of human skeletal muscle to acute bouts of resistance exercise. *J. Appl. Physiol.* **98**, 482–488 (2005).
23. Fujie, T. *et al.* Engineered nanomembranes for directing cellular organization toward flexible biodevices. *Nano Lett.* **13**, 3185–92 (2013).
24. Arber, S., Halder, G. & Caroni, P. Muscle LIM protein, a novel essential regulator of myogenesis, promotes myogenic differentiation. *Cell* **79**, 221–31 (1994).
25. Sung, J. H., Kim, H. S., Jin, H.-J., Choi, H. J. & Chin, I.-J. Nanofibrous membranes prepared by multiwalled carbon nanotube/poly(methyl methacrylate) composites. *Macromolecules* **37**, 9899–902 (2004).
26. Ayutsede, J. *et al.* Carbon nanotube reinforced bombyx mori silk nanofibers by the electrospinning process. *Biomacromolecules* **7**, 208–14 (2006).
27. Sen, R. *et al.* Preparation of single-walled carbon nanotube reinforced polystyrene and polyurethane nanofibers and membranes by electrospinning. *Nano Lett.* **4**, 459–64 (2004).
28. Ko, F. *et al.* Electrospinning of continuous carbon nanotube-filled nanofiber yarns. *Adv. Mater.* **15**, 1161–5 (2003).
29. Voge, C. M., Kariolis, M., MacDonald, R. A. & Stegemann, J. P. Directional conductivity in SWNT-collagen-fibrin composite biomaterials through strain-induced matrix alignment. *J. Biomed. Mater. Res. Part A* **86A**, 269–77 (2008).
30. Namgung, S., Baik, K. Y., Park, J. & Hong, S. Controlling the growth and differentiation of human mesenchymal stem cells by the arrangement of individual carbon nanotubes. *ACS Nano* **5**, 7383–90 (2011).
31. Melechko, A. V., Desikan, R., McKnight, T. E., Klein, K. L. & Rack, P. D. Synthesis of vertically aligned carbon nanofibres for interfacing with live systems. *J. Phys. D: Appl. Phys.* **42**, 193001 (2009).
32. Nguyen-Vu, T. D. B. *et al.* Vertically aligned carbon nanofiber arrays: An advance toward electrical–neural interfaces. *Small* **2**, 89–94 (2006).
33. Yu, Z. *et al.* Vertically aligned carbon nanofiber arrays record electrophysiological signals from hippocampal slices. *Nano Lett.* **7**, 2188–95 (2007).
34. Tosun, Z. & McFetridge, P. S. A composite SWNT–collagen matrix: Characterization and preliminary assessment as a conductive peripheral nerve regeneration matrix. *J. Neural Eng.* **7**, 066002 (2010).
35. de Heer, W. A., Bacsá, W. S., Châtelain, A., Gerfin, T., Humphrey-Baker, R., Forro, L. & Ugarte, D. Aligned carbon nanotube films: Production and optical and electronic properties. *Science* **268**, 845–7 (1995).
36. Reilly, G. C. & Engler, A. J. Intrinsic extracellular matrix properties regulate stem cell differentiation. *J. Biomech.* **43**, 55–62 (2010).
37. Lutolf, M. P., Gilbert, P. M. & Blau, H. M. Designing materials to direct stem-cell fate. *Nature* **462**, 433–41 (2009).
38. Aubin, H. *et al.* Directed 3D cell alignment and elongation in microengineered hydrogels. *Biomaterials* **31**, 6941–51 (2010).
39. Kaji, H., Ishibashi, T., Nagamine, K., Kanzaki, M. & Nishizawa, M. Electrically induced contraction of C2C12 myotubes cultured on a porous membrane-based substrate with muscle tissue-like stiffness. *Biomaterials* **31**, 6981–6 (2010).
40. Nedachi, T., Fujita, H. & Kanzaki, M. Contractile C2C12 myotube model for studying exercise-inducible responses in skeletal muscle. *Am. J. Physiol. Endocrinol. Metab.* **295**, E1191–E204 (2008).
41. Estili, M. & Kawasaki, A. Engineering strong intergraphene shear resistance in multi-walled carbon nanotubes and dramatic tensile improvements. *Adv. Mater.* **22**, 607–10 (2010).
42. Estili, M. *et al.* The homogeneous dispersion of surfactantless, slightly disordered, crystalline, multiwalled carbon nanotubes in α -alumina ceramics for structural reinforcement. *Acta Mater.* **56**, 4070–9 (2008).
43. Ramón-Azcón, J. *et al.* Gelatin methacrylate as a promising hydrogel for 3D microscale organization and proliferation of dielectrophoretically patterned cells. *Lab Chip* **12**, 2959–69 (2012).
44. Wang, D., Fujinami, S., Liu, H., Nakajima, K. & Nishi, T. Investigation of true surface morphology and nanomechanical properties of poly(styrene-*b*-ethylene-co-butylene-*b*-styrene) using nanomechanical mapping: Effects of composition. *Macromolecules* **43**, 9049–55 (2010).
45. Liu, H. *et al.* Quantitative nanomechanical investigation on deformation of poly(lactic acid). *Macromolecules* **45**, 8770–9 (2012).
46. Hutter, J. L. & Bechhoefer, J. Calibration of atomic-force microscope tips. *Rev. Sci. Instrum.* **64**, 1868–73 (1993).



47. Hosseini, V. *et al.* Engineered contractile skeletal muscle tissue on a microgrooved methacrylated gelatin substrate. *Tissue Eng. Part A* **18**, 2453–65 (2012).
48. Obregón, R. *et al.* Non-invasive measurement of glucose uptake of skeletal muscle tissue models using a glucose nanobiosensor. *Biosens. Bioelectron.* **50**, 194–201 (2013).
49. Ahadian, S. *et al.* Interdigitated array of Pt electrodes for electrical stimulation and engineering of aligned muscle tissue. *Lab Chip* **12**, 3491–503 (2012).
50. Ahadian, S. *et al.* A contactless electrical stimulator: application to fabricate functional skeletal muscle tissue. *Biomed. Microdevices* **15**, 109–15 (2013).
51. Ahadian, S. *et al.* Electrical stimulation as a biomimicry tool for regulating muscle cell behavior. *Organogenesis* **9**, 87–92 (2013).
52. Schmittgen, T. D. & Livak, K. J. Analyzing real-time PCR data by the comparative CT method. *Nat. Protocols* **3**, 1101–8 (2008).
53. Hancock, M. J. *et al.* Anisotropic material synthesis by capillary flow in a fluid stripe. *Biomaterials* **32**, 6493–504 (2011).

Acknowledgments

The authors thank the MANA Foundry at NIMS for providing the I-V measurement system. This work was supported by the World Premier International Research Center Initiative (WPI), MEXT, Japan.

Author contributions

S.A. and J.R.-A. conceived the idea and designed the research. S.O. synthesized the GelMA prepolymer. M.E. functionalized the CNTs, prepared the aqueous CNT solutions, and performed the DC conductivity measurements. X.L. helped with the AFM measurements under the supervision of K.N. S.A. and J.R.-A. performed all other experiments, analyzed the results, contributed equally to the work, and wrote the paper. H.S., M.R., H.B., T.M. and A.K. supervised the study. All authors read the manuscript, provided comments, and approved its content.

Additional information

Supplementary information accompanies this paper at <http://www.nature.com/scientificreports>

Competing financial interests: The authors declare no competing financial interests.

How to cite this article: Ahadian, S. *et al.* Hybrid hydrogels containing vertically aligned carbon nanotubes with anisotropic electrical conductivity for muscle myofiber fabrication. *Sci. Rep.* **4**, 4271; DOI:10.1038/srep04271 (2014).



This work is licensed under a Creative Commons Attribution-NonCommercial-ShareAlike 3.0 Unported license. To view a copy of this license, visit <http://creativecommons.org/licenses/by-nc-sa/3.0>